

Mapping co-benefits for carbon storage and biodiversity to inform conservation policy and action

Soto-Navarro C^{*1,2}, Ravilious C¹, Arnell A¹, de Lamo X¹, Harfoot M¹, Hill SLL^{1,3}, Wearn OR⁴, Santoro M⁵, Bouvet A⁶, Mermoz S⁷, Le Toan T⁶, Xia J⁸, Liu S⁹, Yuan W^{10,11}, Spawn SA^{12,13}, Gibbs HK^{12,13}, Ferrier S¹⁴, Harwood T¹⁴, Alkemade R¹⁵, Schipper AM^{15,16}, Schmidt-Traub G¹⁷, Strassburg B¹⁸, Miles L¹, Burgess ND^{1,19}, Kapos V¹

¹UN Environment Programme World Conservation Monitoring Centre (UNEP-WCMC), 219 Huntingdon Road, Cambridge, CB3 0DL, United Kingdom.

²Luc Hoffmann Institute, Rue Mauverney 28, 1196, Gland, Switzerland.

³Natural History Museum, Cromwell Road, London, SW7 5BD, United Kingdom.

⁴Institute of Zoology, Zoological Society of London, Regent's Park, London, NW1 4RY, United Kingdom.

⁵Gamma Remote Sensing, Worbstrasse 225, 3073, Gümligen, Switzerland.

⁶CESBIO, Edouard Belin, 31401, Toulouse, France.

⁷GlobEo, Avenue Saint-Exupéry, 31400, Toulouse, France.

⁸Tianjin Key Laboratory of Water Resources and Environment, Tianjin Normal University, Tianjin 300387, China.

⁹National Engineering Laboratory for Applied Technology of Forestry & Ecology in Southern China, and College of Biological Science and Technology, Central South University of Forest and Technology, Changsha 410004, China.

¹⁰State Key Laboratory of Earth Surface Processes and Resource Ecology, Beijing Normal University, Beijing 100875, China.

¹¹State Key Laboratory of Cryospheric Sciences, Cold and Arid Regions Environmental and Engineering Research Institute, Chinese Academy of Sciences, Lanzhou 730000, China.

¹²Department of Geography, University of Wisconsin-Madison, Madison, Wisconsin, United States.

¹³Centre for Sustainability and the Global Environment, University of Wisconsin-Madison, Madison, Wisconsin, United States.

¹⁴CSIRO, GPO BOX 1700, Canberra, Australia.

¹⁵PBL Netherlands Environmental Assessment Agency, PO Box 30314, 2500 GH The Hague, Netherlands.

¹⁶Radboud University, Department of Environmental Science, PO Box 9010, 6500 GL Nijmegen, Netherlands.

¹⁷UN Sustainable Development Solutions Network, 75009, Paris, France.

¹⁸International Institute for Sustainability (IIS), CEP: 22460-320, Rio de Janeiro, Brazil.

¹⁹Centre for Macroecology, Evolution and Climate, The Natural History Museum, University of Copenhagen, Copenhagen, Denmark.

Supplementary Information

Methods

Carbon data

We undertook a literature review to search for and review existing datasets on biomass and soil organic carbon in terrestrial ecosystems using peer-reviewed journal articles and reports. We selected search terms in English to provide a broad, but manageable coverage of regional and global spatially-explicit information of carbon stocks in terrestrial ecosystems (Table 1). We also identified additional datasets through our network of contacts and expert knowledge of biomass and soil datasets. We were only interested in studies that (a) described published spatial datasets for carbon in terrestrial

ecosystems (above/below-ground biomass, soil organic carbon) or (b) provided new estimates for carbon stocks for terrestrial ecosystems at large scale (for the purposes of comparison with spatial data).

We evaluated the datasets identified against existing knowledge and compared them with each other using a set of criteria that included resolution, accuracy, biomass definition and date to help determine which datasets to combine to produce the global map. We particularly focused on identifying and assessing datasets that covered areas and biomass carbon stocks where detailed spatial data was lacking from known global maps, such as non-forest biomass in temperate and boreal areas, and where biomass may have been underrepresented in existing assessments. We preferred coarser regional dataset over higher resolution data covering only a limited area in order to present as seamless and accurate a carbon map as possible that most reliably represented biomass and soil carbon distribution across the globe.

We created the global carbon map by overlaying the selected carbon datasets with the ESA CCI Landcover map for the year 2010 [42], assigning each grid cell the corresponding biomass value from the biomass map associated with the grid cell's landcover type. Each dataset was aggregated to a nominal scale of 300 m resolution. Forest categories in the CCI ESA 2010 landcover dataset were used to extract above-ground biomass from Santoro et al. (2018) [71] for forest areas. Woodland and savanna biomass were then incorporated for Africa from Bouvet et al. (2018) [85]. We added above-ground woody biomass for areas outside of Africa and outside of forest from Santoro et al. (2018) [71]. We also incorporated grassland areas from Xia et al. (2014) [80] and Spawn et al. (2017) [82] datasets averaged by ecological zone for each landcover type. Specifically, these were croplands, sparse vegetation, grassland (pixels within the CCI ESA 2010 landcover missing from Xia et al. (2014) [80]) and areas of shrubland outside of Africa that were missing from Santoro et al. (2018) [71]. This completed the assemblage of the above-ground biomass map. We then added below-ground biomass using root-to-shoot ratios from the 2006 IPCC guidelines for National Greenhouse Gas Inventories [88]. No below-ground values were assigned to croplands as ratios were unavailable. Above- and below-ground biomass were then summed together and multiplied by 0.5 to convert to carbon, generating a single above-and-below-ground biomass carbon layer (Figure S1). Finally, we summed the above- and below-ground biomass carbon and soil carbon (to 1 m depth) to generate the combined "total" carbon layer.

Biodiversity data

We included in our species component of biodiversity a metric based on rarity-weighted richness (RWR) [89] as a proxy for biodiversity importance (and arguably endemism) and aggregated the scores from all species. The logic for this is that greater the importance of the grid cell for contributing to each species' total geographic range, the more biodiversity is at risk if that region is degraded. We rasterised species range data at 10 arc-seconds (approximately 300m at the equator) from IUCN Red List polygons (IUCN 2017), using Google Earth Engine, and we aggregated at 1 km. We also refined each species' range by removing areas of unsuitable land cover [42], using information on species' habitat preferences (IUCN 2017). Areas outside the species' known altitudinal limits (IUCN 2017) were also removed using elevation data [90]. We scored each grid cell of the species' refined range

based on the range-size rarity for each species (the proportion of the species' global AOH the cell represents). Thus, species with smaller ESHs have larger scores per grid cell they occur in. For each cell in the final dataset we then calculated a total score, by summing scores across all the species (potentially) occurring in it.

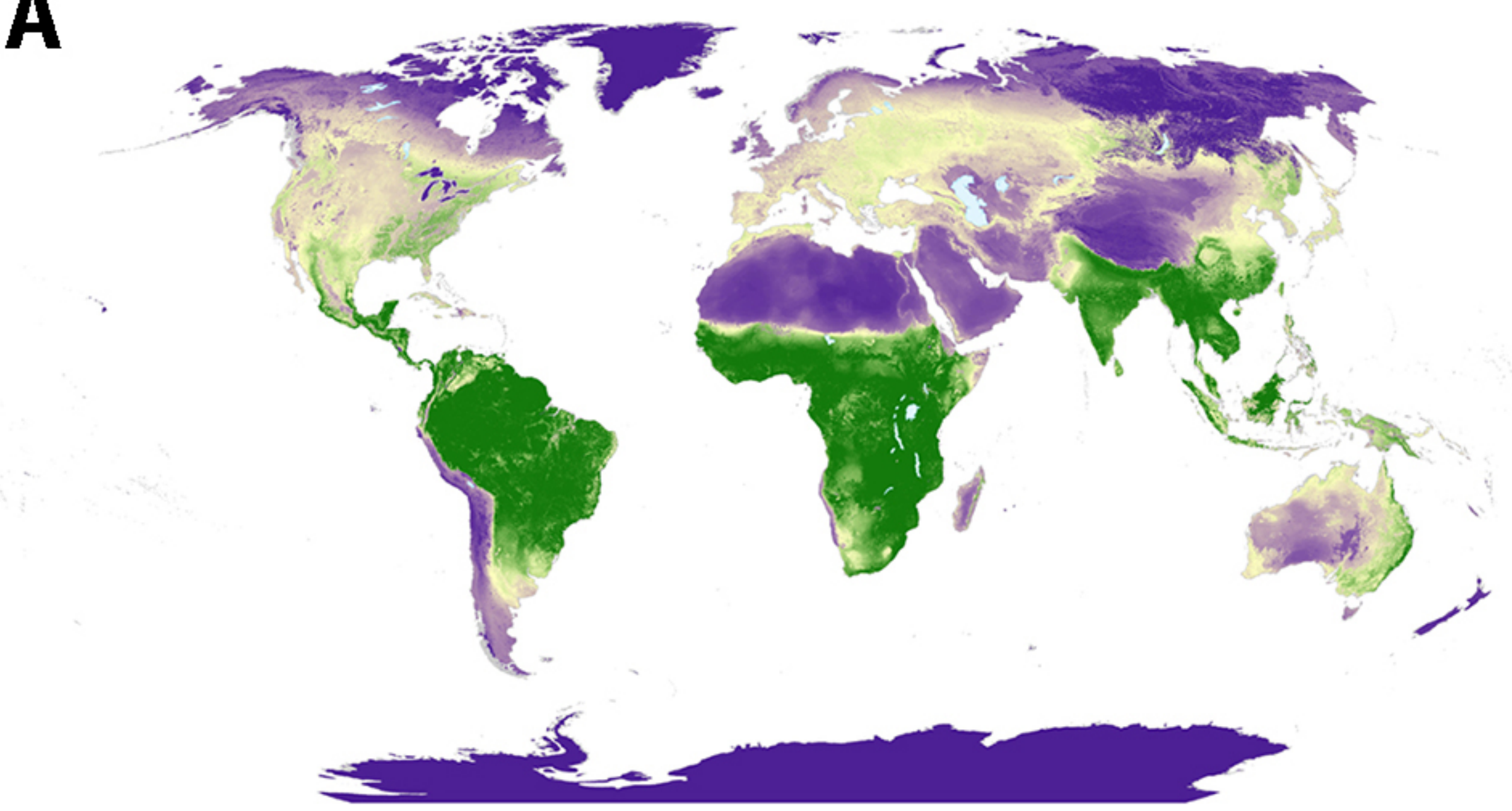
GLOBIO's MSA provides a measure on the compositional integrity or intactness of local communities within a pixel. It represents the mean abundance of original species in relation to a particular pressure as compared to the mean abundance in an undisturbed reference situation. Pressures include climate change, atmospheric nitrogen deposition, land use, infrastructure, habitat fragmentation and hunting (in tropical regions). A pixel with a MSA of 1 means a biodiversity that is similar to the natural situation, whilst a MSA close to 0 means a completely destroyed ecosystem, with no original species remaining. We used a 300m MSA map for 2015 derived from GLOBIO4 [83] aggregated at 1km resolution.

The PREDICTS's BII also provides a measure of the intactness of ecological assemblages and it represents the average community abundance of the originally present species, as affected by four pressure variables, i.e., land use, land-use intensity, human population density, and proximity to the nearest road, in the pixel (relative to the original state assuming pristine vegetation with minimal human influence). We used for the analyses the 1 km global map of the Biodiversity Intactness Index from Newbold et al. (2016) [47].

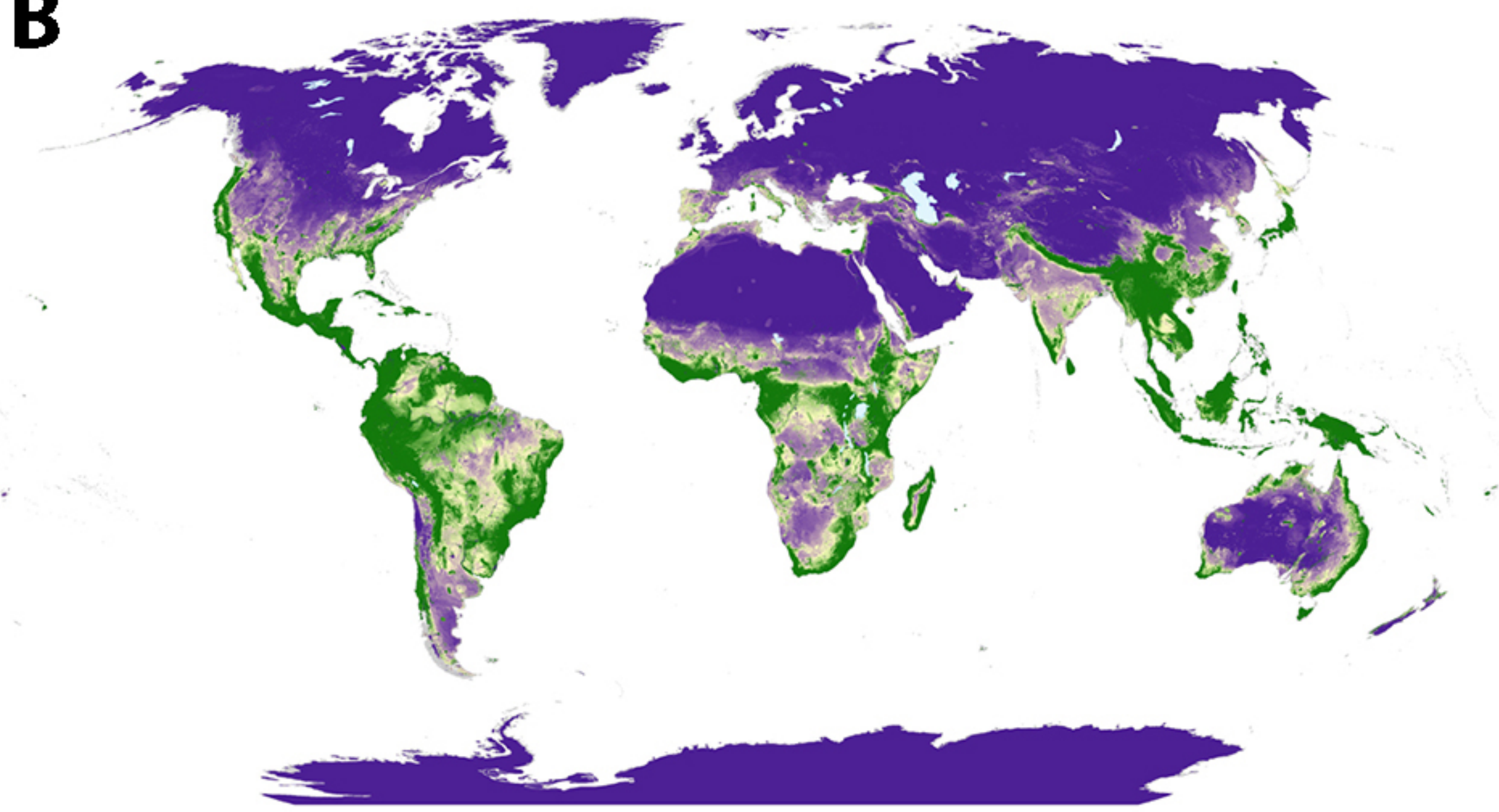
The CSIRO Biodiversity Habitat Index (BHI) estimates the impacts of habitat transformation on retention of terrestrial biodiversity [91]. It integrates: 1) habitat condition, on a scale of 0 to 1, derived from statistical downscaling of coarse-resolution land-use data using 1km resolution environmental and remotely-sensed land-cover covariates; and 2) spatial turnover in species composition (temporal beta diversity) of vascular plant communities modelled as a function of species occurrence records and 1km resolution climate, terrain and soil surfaces. The BHI score assigned to a given 1km cell is calculated as the average condition of all cells predicted to have supported a similar composition of species to the cell of interest (prior to habitat transformation). A score of 0 means that that no intact habitat remains across compositionally similar cells, while a score of 1 indicates that the habitat of these cells remains completely intact. We used the Biodiversity Habitat Index at 1km resolution for vascular plants for 2015.

Figure S1. Global biodiversity datasets used to calculate BIp and BIr. A) Species richness–AOH (Area of Habitat) and B) Rarity-weighted richness–AOH for mammals, birds and amphibians, C) Biodiversity Intactness Index (PREDICTS), D) Mean Species Abundance (GLOBIO4) and E) Biodiversity Habitat Index (CSIRO).

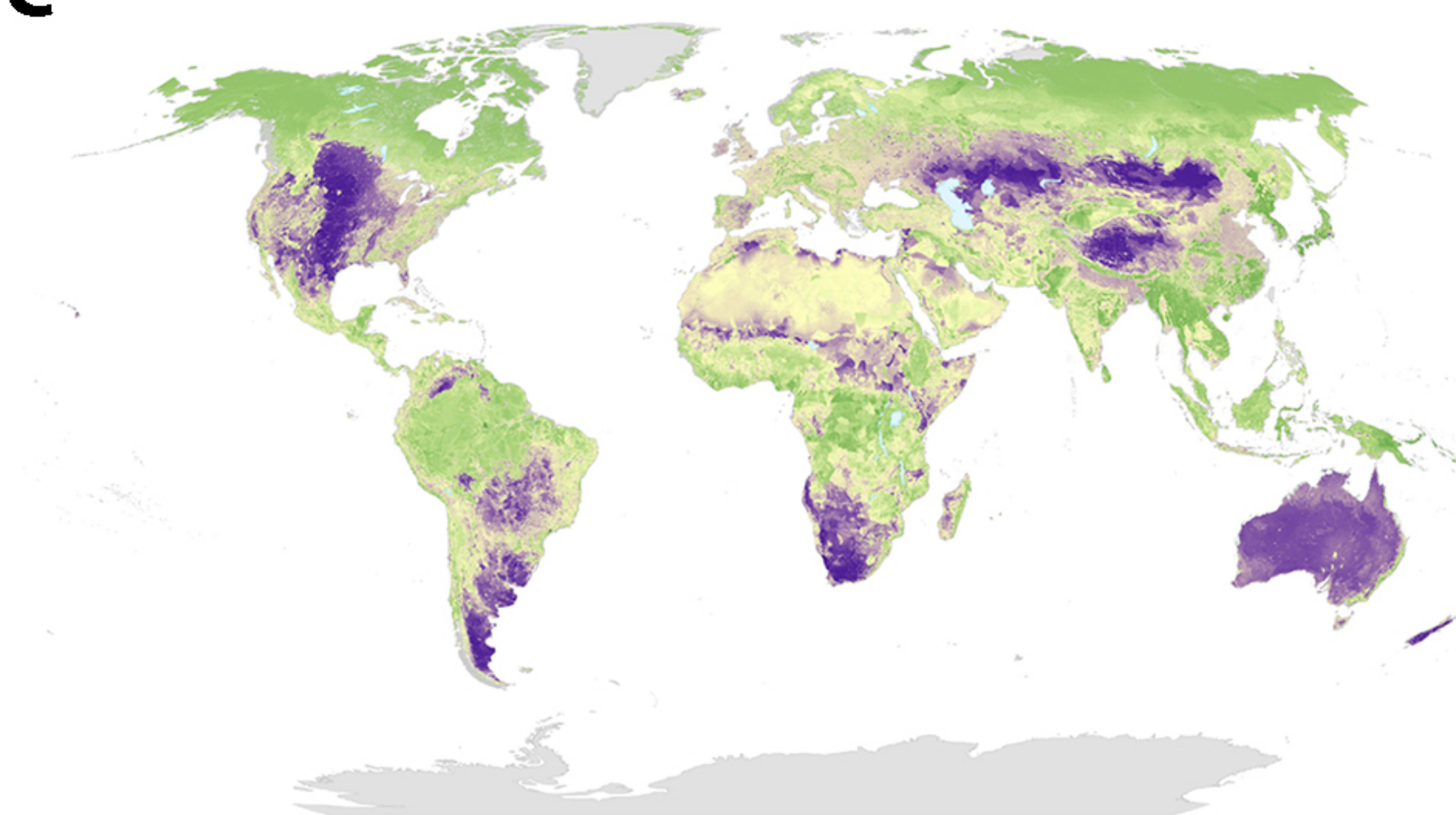
A



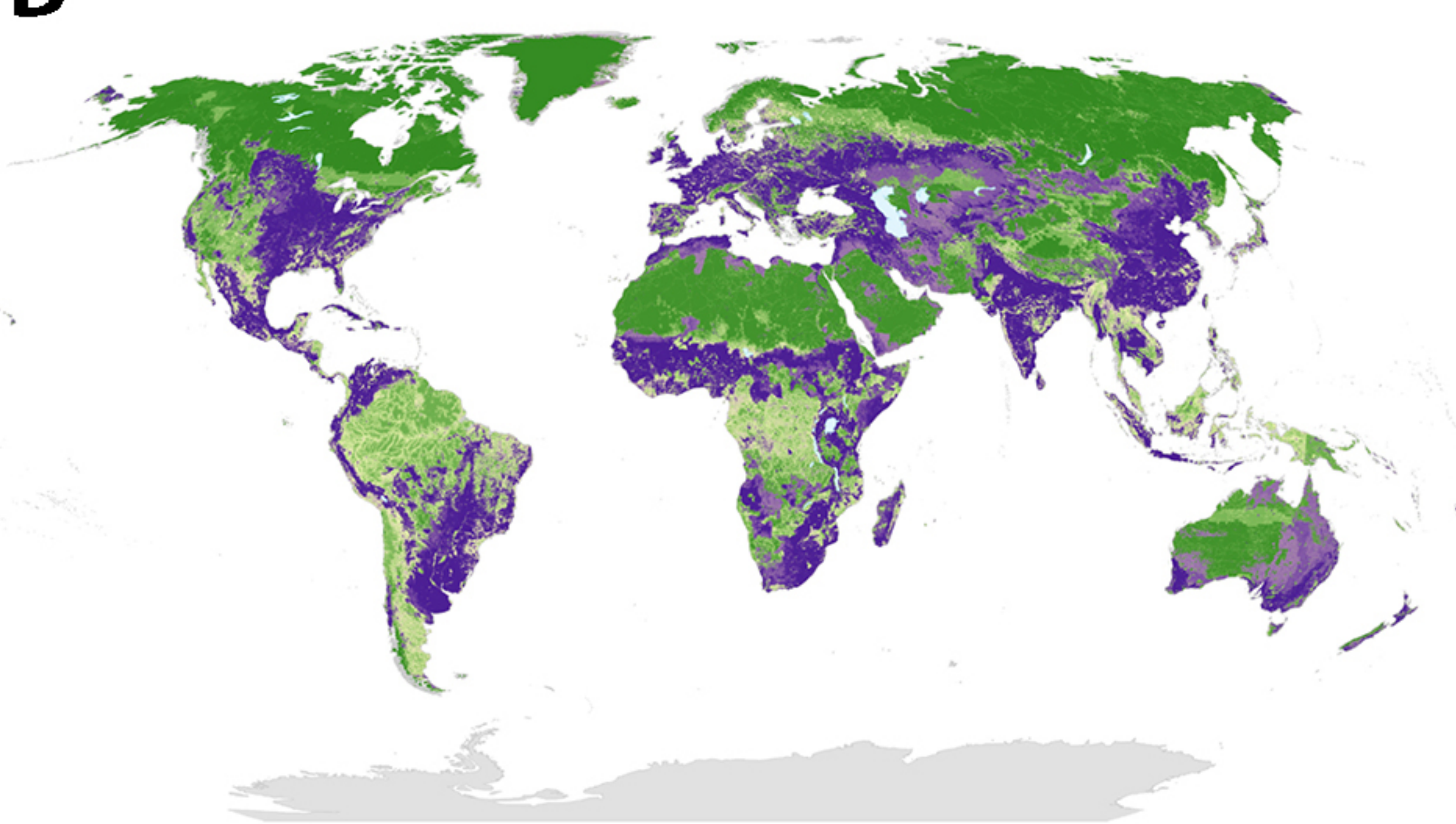
B



C



D



E

